Chemical Science

RSC Publishing

EDGE ARTICLE

View Article Online
View Journal | View Issue

Cite this: *Chem. Sci.*, 2013, **4**, 3232

Metal-organic frameworks displaying single crystal-to-single crystal transformation through postsynthetic uptake of metal clusters†

Jia Li, Peng Huang, Xue-Ru Wu, Jun Tao,* Rong-Bin Huang and Lan-Sun Zheng

Three metal-organic frameworks (MOFs) formulated as $[Co_3O(BTB)_2(H_2O)_x(DMF)_y]\cdot zDMF\cdot nH_2O$ (BTB = 1,3,5-benzenetribenzoate; **1a**, $x = y = 1, z = 7.5, n = 12$; **1b**, $x = 2, y = 0, z = 8.5, n = 8$; **1c**, $x = 2, y = 1, z = 7, n = 8$) have been synthesized under different temperatures; they crystallize as two-fold interpenetrated analogous structures with the same structural trinuclear $Co_3O(CO_2)_6$ secondary building units (SBUs), and their stabilities depend on the temperature under which they formed. Upon immersion in the filtrate of **1a** (namely **1a-s**, freshly filtered) or **1b** (namely **1b-s**, filtered and then activated in air for three days), single crystal-to-single crystal (SCSC) transformations of **1a–1c** to a new MOF, formulated as $[Co_6O_2(OH)_4(BTB)_{8/3}(H_2O)_4]\cdot 14DMF\cdot 4EtOH\cdot 2H_2O$ (**2**), occur along with dramatic color change from blue purple to red. Crystallographic studies reveal that the new MOF is also two-fold interpenetrated but is constructed with hexanuclear $Co_6O_2(CO_2)_8$ SBUs. This SCSC transformation from **1a–1c** to **2** can take place only in **1a-s** or **1b-s** but not in **1c-s** and is accompanied with an increase of metal-to-ligand ratio. ESI-MS studies unveil the formation of free $\{Co_3O\}$ units *in situ* formed only in **1a-s** and **1b-s**, and evidence that the SCSC transformation involves a postsynthetic uptake of free metal clusters, $\{Co_3O\}$. On the other hand, the SCSC transformation speed decreases from **1a** to **1c**, which is determined by the chelate carboxylate groups undergoing cleavage of metal-carboxylate bonds during the SCSC transformation and the shape of the 1D channels affecting the diffusion of free metal clusters. Furthermore, the resulting MOF (**2**) can maintain its crystallinity upon activation and adsorbs iodine up to 38 wt%. Combined with the significant SCSC transformation through postsynthetic uptake of free metal clusters and the resulting MOF capable of adsorbing iodine, the present approach not only provides a true route to construct SBUs-based MOF materials with pre-existing "real" SBUs but also represent a new type of SCSC transformation in the field of MOFs that is able to efficiently tune structures and physicochemical properties of MOFs in the solid states.

Received 17th May 2013
Accepted 28th May 2013

DOI: 10.1039/c3sc51379c

www.rsc.org/chemicalscience

Introduction

Metal-organic frameworks have attracted much interest in the last decade due to their promising applications for gas storage/separation,[1] catalysis,[2] luminescence,[3] drug delivery,[4] sensors[5] and magnetic materials.[6] From the structural point of view, the successful construction of MOFs usually depends on the rational selection of polytopic ligands, metal ions or secondary building units (SBUs) as well as reaction conditions. Through extensive studies in recent years, thousands of MOFs with desired and various topological structures have been synthesized, in which the targeted SBUs are proven to be crucial because they usually act as structure-directing entities. Currently, three typical metal clusters $M_2(O_2CR)_4L_2$ (M = Cu, Zn; L = terminal ligand),[7] $Zn_4O(O_2CR)_6$,[8] and $M_3(\mu_3\text{-}O)(O_2CR)_6L_3$ (M = Cr, Fe, Ni, Co)[9,10] have been widely utilized as square, octahedral and trigonal prismatic SBUs, respectively, which are connected through polytopic linkers to produce various MOFs. However, defining these SBUs in fact stems from a deconstructing demand, it is still unclear whether these SBUs, in particular their core structures such as $\{Co_3(\mu_3\text{-}O)\}$, can form solely before constructing MOFs.

On the other hand, among the known MOFs some can undergo single-crystal to single-crystal (SCSC) transformations,[11–15] and the driving forces for SCSC transformation vary from heat,[11] light,[12] redox reactions,[13] sorption/desorption or rearrangement of guest molecules[14,15] to postsynthetic modification (PSM).[16] Through SCSC transformations, new MOFs that can not be formed under conventional conditions may be easily obtained in high yield. However, an SCSC transformation of MOFs is still difficult to achieve, partly because SCSC transformation in the solid state can barely realize regarding to the cleavage and formation of bonds

State Key Laboratory of Physical Chemistry of Solid Surfaces and Department of Chemistry, College of Chemistry and Chemical Engineering, Xiamen University, Xiamen 361005, People's Republic of China. E-mail: taojun@xmu.edu.cn; Fax: +86-592-2188138; Tel: +86-592-2183047

† Electronic supplementary information (ESI) available: Information of materials and measurements, synthesis and characterization data, supplementary figures, TG and IR. CCDC 890975–890978. For ESI and crystallographic data in CIF or other electronic format see DOI: 10.1039/c3sc51379c

simultaneously occurred in more than one direction, and/or hardly retains crystallinity after the solid-state rearrangement of atoms. Fortunately, postsynthetic methods may satisfy these requirements[16] even though in some cases the transformation is incomplete.[17] Postsynthetic methods are developed to modify and functionalize the chemical and physical properties of MOFs and certainly their structures. They are particularly attractive for a couple of advantages, for example, to overcome the limitation of achieving multifunctional MOFs by direct synthesis from solvothermal methods commonly used to prepare MOFs and to engender both the interior and exterior of MOFs materials with new properties by selective metal or ligand addition/exchange and/or organic transformations or reactions. Strictly speaking, PSM precludes the noncovalent/noncoordinate postsynthetic transformations and thus can be divided into five areas: (a) addition of metal ions to free ligand sites or ligands to unsaturated metal sites, (b) metal-ion or ligand exchange, (c) covalent PSM, (d) dative PSM, and (e) postsynthetic deprotection.[16] In these cases, the core structures of SBUs in MOFs almost remain unaltered and therefore the MOFs' frameworks change little.

Besides, searching new applications for MOFs is a consecutive task, which has seen the advances in iodine sorption by MOFs. The use of MOFs for iodine sorption is firstly motivated by the capturing, enrichment and sequestering of the volatile radioactive iodine produced in nuclear energy enterprises; for this purpose, some MOFs have been tested for their capabilities for capturing iodine in solution and low-pressure vapor,[18] among which activated ZIF-8 (ref. 18*a*) shows highly efficient sorption of iodine (120 wt% I_2) and pressure amorphization-enhanced iodine retention and storage. Another motivation is based on the particular chemistry of iodine, to form polyiodides upon sorption,[19] which therefore engender MOFs with new properties such as conductivity and nonlinear optical activity.[20] Iodine sorption can also carry out dative PSM of MOFs, in a particular case, an oxidative addition reaction involving electron transfer from Pt^{II} ions to iodine molecules and cleavage of the molecular iodine bond undergoes within a spin-crossover MOF $\{Fe(pz)[Pt^{II}(CN)_4]\}$[21] when iodine molecules diffuse into the pores, and resulting in the formation of iodine adduct $\{Fe(pz)[Pt^{II/IV}(CN)_4(I)]\}$ with Pt–I bonds. This modification has precisely controlled and consecutively modulated the spin transition temperature of this spin-crossover MOF.

In this paper, we report three two-fold interpenetrated 3D MOFs, **1a–1c**, based on oxo-centered trinuclear $Co_3O(CO_2)_6$ SBUs, which undergo SCSC transformation in the filtrate of **1a** or **1b** to give a new two-fold interpenetrated 3D MOF **2** with hexanuclear $Co_6O_2(CO_2)_8$ SBUs. This transformation is unexpectedly realized through postsynthetic uptake of free Co_3O units in solution, and resulting in an expansion of SBUs from trinuclear to hexanuclear and an increase of metal-to-ligand ratio. Unlike **1a–1c** that lose crystallinity upon activation, the resulting MOF **2** can maintain its crystallinity upon activation and adsorbs iodine up to 38 wt%. The present approach not only provides a true route to construct SBU-based MOF materials with pre-existing "real" SBUs but also represents new type of SCSC transformation and PSM that are able to efficiently tune structures and physicochemical properties of MOFs in the solid states.

Results and discussion

Structural characterization

Single-crystal X-ray diffraction studies revealed that **1a–1c** crystallized in the orthorhombic space group *Pnma*, having 2-fold self-interpenetrated 3D frameworks based on $Co_3O(CO_2)_6$ SBUs, which show slight differences among **1a–1c** (Fig. S1–S3, ESI†). Besides the μ_3-O^{2-} ion and carboxylate groups, Co1 is bridged to its symmetry-related one by a water molecule in **1a** or **1b**, while which in **1c** are terminally coordinated by water molecules, the coordination sphere of Co2 is completed by DMF, water and DMF molecule in **1a**, **1b** and **1c**, respectively. Therefore, complexes **1a–1c** are slightly different in the framework compositions, giving formulae of $[Co^{III}_2Co^{II}(\mu_3\text{-}O)(DMF)(H_2O)(BTB)_2]\cdot(DMF)_{7.5}(H_2O)_{12}$ (**1a**), $[Co^{III}_2Co^{II}(\mu_3\text{-}O)(H_2O)_2(BTB)_2]\cdot(DMF)_{8.5}(H_2O)_8$ (**1b**), and $[Co^{III}_2Co^{II}(\mu_3\text{-}O)(DMF)(H_2O)_2(BTB)_2]\cdot(DMF)_7(H_2O)_8$ (**1c**), respectively, where the amounts of guest solvent molecules are determined by considering the elemental analysis and thermogravimetric results (ESI†). In **1a–1c**, the 3D frameworks are self-interpenetrated and exhibit 1D channels running along the *a* axis (Fig. 1a–c), the trigonal prismatic $Co_3O(CO_2)_6$ SBUs are connected to each other *via* the triangular BTB skeletons to yield (3,6)-connected frameworks (Fig. 1d). Unfortunately, we cannot determine the crystal structures of **1a** and **1b** at higher temperatures because of their poor stability. But interestingly, **1c** shows thermochromism and temperature-induced transformations between 100 and 290 K, which are similar to the breathing materials MIL-47 and MOF-39.[26] As the temperature increases, the space group remains unaltered while the shapes of the 1D channels change from diamond to square (Table 1).

Complex **2**, $[Co_6O_2(OH)_4(BTB)_{8/3}(H_2O)_4]\cdot14DMF\cdot4EtOH\cdot2H_2O$, crystallizes in the cubic space group $Im\bar{3}$ and is also 2-fold self interpenetrated (Fig. 2a). The framework is based on new SBUs, $Co_6O_2(CO_2)_8$, which can be viewed as double $Co_3O(CO_2)_4$ entities bridged by hydroxyl groups (Fig. S4, ESI†). Each cuboidal

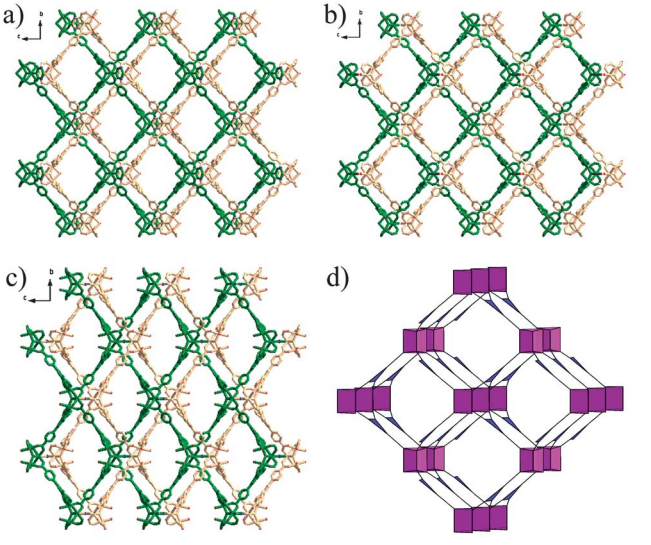

Fig. 1 Perspective view of the interpenetrated 3D frameworks (a–c) and topological structure (d) of **1a–1c**.

Co_6 SBU connects eight trigonal BTB ligands, and each BTB ligand in turn connects three Co_6 SBUs, thus forming a (3,8)-connected 3D framework (Fig. 2b).[22] Although, being 2-fold self interpenetrated, all complexes are highly porous, the accessible volumes are 60.4%, 60.3%, 58.6% and 61.2% per unit cell for **1a**, **1b**, **1c** and **2**, respectively, as calculated using PLATON.[23]

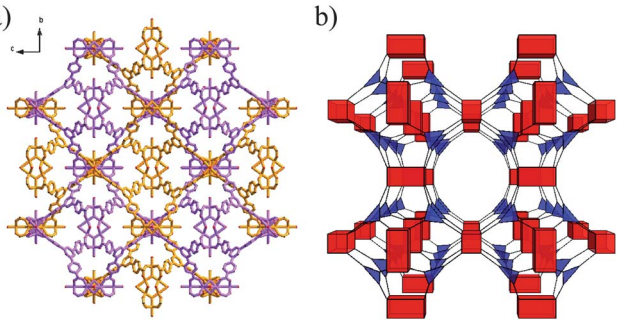

Fig. 2 Perspective view of the self-interpenetrated 3D framework (a) and topological structure (b) of **2**.

SCSC transformation

The reaction of H_3BTB with cobalt(II) salts in DMF-EtOH under various temperature generated purple single crystals of **1a** (room temperature), **1b** (40 and then 90 °C) and **1c** (70 and then 110 °C), leaving solutions **1a-s**, **1b-s** and **1c-s** after filtration, respectively. All crystals (**1a–1c**) showed no differences in morphology, color and transparency, their space groups were also the same but the unit-cell volumes decreased from **1a** to **1c** by ~3% (Table S1, ESI†). The main difference lies in their sensitivity to air; **1a** cracked soon after leaving the mother liquor while **1b** was more stable than **1a**, and **1c** was the most stable one. Unexpectedly, when as-synthesized **1a** crystals (Fig. 3a) were immersed again in fresh filtrate **1a-s**, the SCSC transformation began to occur and they completely converted into new crystals of **2** (Fig. 3b) in two months, accompanied by color changes for both crystals and solution (Fig. 3c), while the crushed **1a** crystals immersed in fresh filtrate **1a-s** completed the SCSC transformation within only one week, the completeness was confirmed by PXRD (Fig. S5–S6, ESI†). The complete transformation from crashed **1b** or **1c** crystals to **2** crystals in fresh filtrate **1a-s** needed longer time, *i.e.* ~three weeks for **1b**

Table 1 Temperature-dependent crystallographic data of **1c**

	1c				
T/K	100	120	140	160	180
					
Cryst. syst.			Orthorhombic		
Space group			*Pnma*		
a/Å	17.4883(6)	17.4474(3)	17.4730(6)	17.4692(6)	17.4280(4)
b/Å	27.5596(19)	27.5264(10)	27.5347(17)	27.5594(16)	27.5847(11)
c/Å	18.8181(15)	18.8060(9)	18.8196(15)	18.8257(15)	18.8087(13)
V/Å	9069.8(10)	9031.8(6)	9054.4(10)	9063.5(9)	9042.2(8)
R_1/wR_2	0.0884/0.2584	0.0774/0.2108	0.0904/0.2671	0.0901/0.2584	0.0872/0.2410
					
	200	230	250	270	290
T/K					
Cryst. syst.			Orthorhombic		
Space group			*Pnma*		
a/Å	17.4516(4)	17.4940(4)	17.4362(12)	17.426(2)	17.2514(19)
b/Å	27.5162(13)	27.0815(9)	25.136(2)	25.294(6)	24.999(7)
c/Å	19.0369(19)	19.6022(7)	22.475(2)	21.889(4)	21.297(5)
V/Å	9141.6(10)	9286.8(5)	9850.3(14)	9648.0(3)	9185(4)
R_1/wR_2	0.1081/0.3083	0.0676/0.2067	0.0840/0.2052	0.0986/0.2288	0.0942/0.2234
					

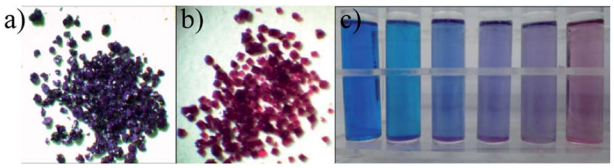

Fig. 3 Morphology of crystals **1a** (a) and **2** (b), and the transformation process showing color changes (c).

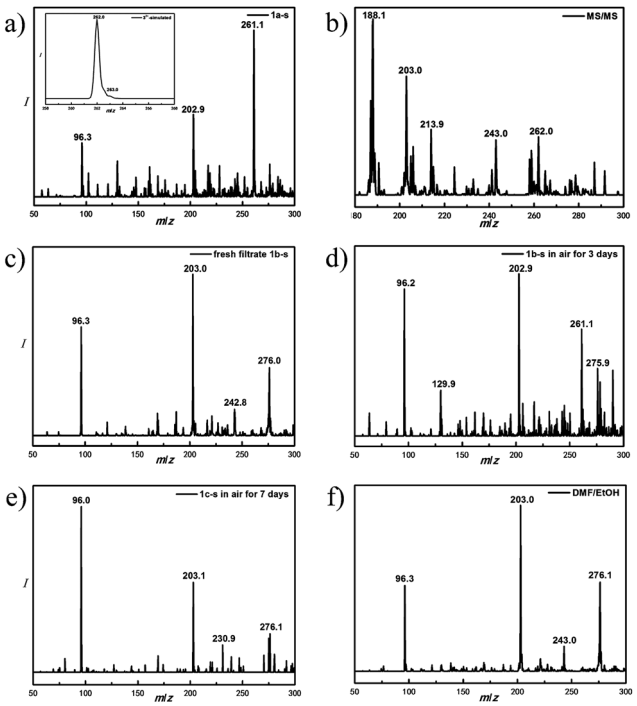

Fig. 4 ESI-MS measurements of **1a-s** (a), the simulated isotropic distribution of m/z = 262.0 for $[Co^{III}_2Co^{II}(\mu_3\text{-}O)(OH)_4(DMF)_2(EtOH)(H_2O)_4]^{2+}$ (a, inset), the tandem mass spectrometry of m/z = 261.1 (b), the fresh filtrate **1b-s** (c) and that opened in air for three days (d), **1c-s** opened in air for seven days (e) and DMF/EtOH mixture for comparison (f).

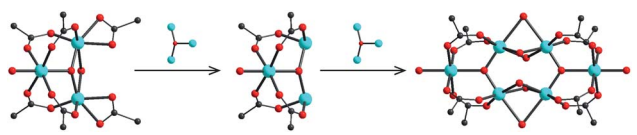

Fig. 5 The transformation of SBUs from **1a–1c** to **2** involving the cleavage and formation of Co–O bonds induced by uptake of free $\mathbf{3}^{2+}$ cluster.

and more than two months for **1c**, respectively. Interestingly, by immersing crushed **1a**, **1b** or **1c** crystals in fresh filtrate **1b-s**, the transformation could not take place, instead it could occur in the **1b-s** that had been opened in air for at least 3 days. While no transformation had been found by immersing crushed **1a**, **1b** or **1c** crystals in **1c-s**, whatever it was fresh filtrate or not.

By careful analysis of the SCSC transformation process, two specific points can be summarized: (1) crystals **1a–1c** are all able to undergo transformation, but with transformation speed **1a** > **1b** > **1c**; and (2) the transformation takes place only in the solution **1a-s** or **1b-s** (having been opened in air for several days). From the structural point of view, **1a–1c** possess similar framework structures and SBUs, in which a common feature is

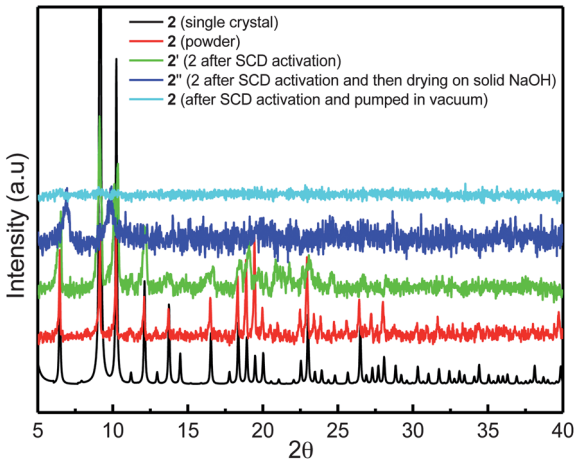

Fig. 6 PXRD patterns of 2 and its activated products.

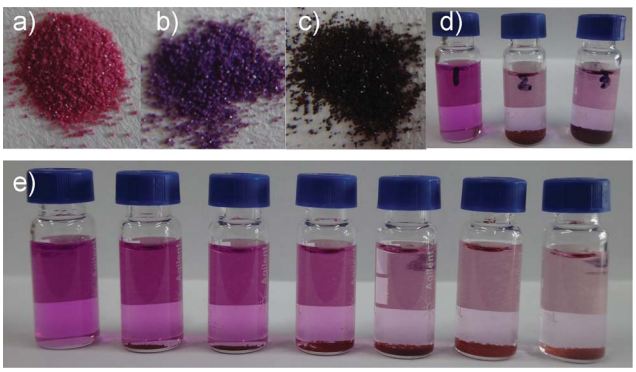

Fig. 7 The crystalline products of **2′** (a), **2′′** (b) and **2′′′** (c), adsorption of I_2 in 1.5 mL cyclohexane solution (0.5 mg I_2) by the same amount of **2′**and **2′′** (10 mg of each) within 36 h, (d) 1: blank, 2: **2′**, 3: **2′′**), and adsorption of I_2 by **2′** in cyclohexane (0.5 mg I_2/1.5 mL) within 3 days with sample weight of 0, 2, 3, 5, 7, 10 and 15 mg, respectively, from left to right (e).

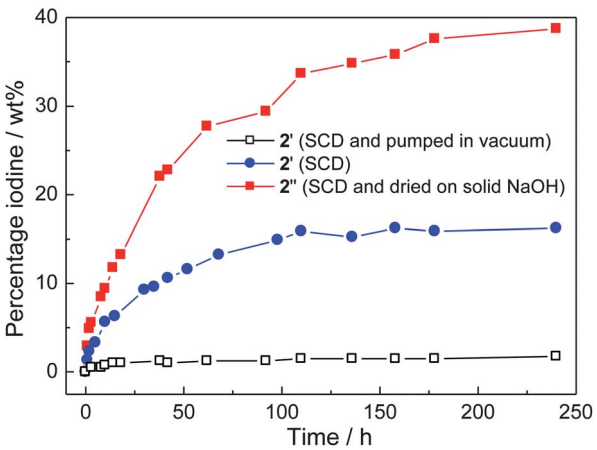

Fig. 8 Gravimetric uptake of iodine by activated **2** as a function of time at 30 °C.

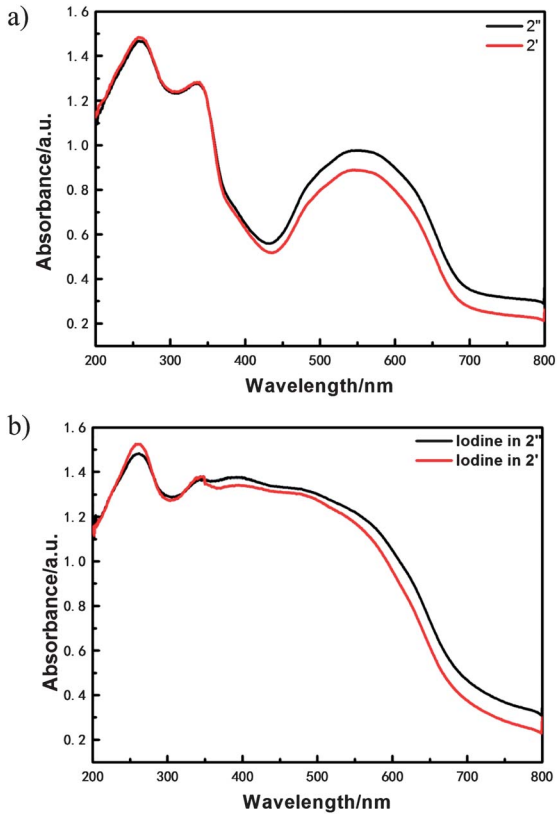

Fig. 9 UV-visible spectra of **2′** and **2′′** (a) and iodine-doped **2′** and **2′′** (b) in the reflectance mode in the solid states, respectively.

that the coordination bonds involving the chelating carboxylate groups (Co1–O1 and Co1–O2 in Fig. S1–S3 and Table S2, ESI†) break during SCSC transformation, thus **1a–1c** show similar SCSC transformation behavior. However, the O1–Co1–O2 bond angles for **1a**, **1b** and **1c** are 57.4(3), 58.7(3) and 59.3(1)°, respectively, which indicate that the tension of the chelate carboxylate group follows the sequence **1a** > **1b** > **1c**, in accord with the transformation speed. This result also confirms that solvothermal synthesis at higher temperature brings about a more stable product. On the other hand, the dimensions of the 1D channels (Fig. 1a–c), assumed to be $b \times c$, for **1a–1c** at 173 K are 25.629(5) × 20.800(4) Å^2, 25.347(2) × 20.880(2) Å^2, 27.758(6) × 18.762(4) Å^2, respectively. The narrow 1D channel, *e.g.* **1c**, restricts the free diffusion of metal clusters (see below) into the channel, which undeniably influences the diffusion-determining transformation speed. Therefore, the speed of transformation is probably controlled by both the tension of chelating carboxylato groups and the shape of the 1D channels.

In order to elucidate the second point, one should note that the transformation from **1a–1c** to **2** involves an increase of metal-to-ligand ratio. However, immersing crushed **1a–1c** crystals in either DMF–EtOH solution of $CoCl_2$ or pure DMF–EtOH showed no transformation, which means that the transformation is not induced by the uptake of free metal ions or loss of BTB ligands. On the other hand, the transformation could take place in **1a-s** (fresh filtrate) or **1b-s** (having been placed in air for several days), but could not in **1c-s**. So there must be something different among the three solutions. Electrospray ionization mass spectrometry (ESI-MS) studies revealed that **1a-s** (fresh filtrate) and **1b-s** (opened in air for three days) contained a common peak of m/z = 261.1 (Fig. 4a and d), while fresh filtrate **1b-s** and **1c-s** did not (Fig. 4c and e). Recalling that the structural units have been expanded from Co_3O in **1a–1c** to Co_6O_2 in **2**, this peak is most probably corresponding to the $[Co^{III}_2Co^{II}(\mu_3\text{-}O)(OH)_4(DMF)_2(EtOH)(H_2O)_4]^{2+}$ species ($\mathbf{3}^{2+}$, m/z = 262.0). The simulated isotropic distribution (Fig. 4a, inset) based on this formula is in line with the experimental data, the tandem mass spectrometry[24] of this peak (Fig. 4b) shows five peaks (m/z) at 188.1, 203.0, 213.9, 243.0 and 262.0, which correspond to $[Co^{III}_2Co^{II}(\mu_3\text{-}O)(OH)_4(EtOH)(H_2O)_4]^{2+}$ (m/z = 188.9), $[Co^{III}_2Co^{II}(\mu_3\text{-}O)(OH)_4(DMF)(H_2O)_4]^{2+}$ (m/z = 203.0), $[Co^{III}_2Co^{II}(\mu_3\text{-}O)(OH)_4(DMF)_2(H_2O)]^{2+}$ (m/z = 212.5), $[Co^{III}_2Co^{II}(\mu_3\text{-}O)(OH)_4(DMF)_2(EtOH)(H_2O)2]^{2+}$ (m/z = 244.0) and $\mathbf{3}^{2+}$, respectively. These results hint that the free cationic species $\mathbf{3}^{2+}$ could be stable in solution and its formation was related to dioxygen in air. During the synthesis of **1a**, dioxygen may leak into the reaction system to oxidize Co(II) and $\mathbf{3}^{2+}$ forms at extremely slow speed so that the formation of **1a** takes place only at four months later when the concentration of $\mathbf{3}^{2+}$ arrives at a certain level, so the remaining $\mathbf{3}^{2+}$ in fresh **1a-s** can be detected by ESI-MS. Meanwhile, the **1a** crystals in the undisturbed reaction system can also subsequently transfer to **2**, which indicates that $\mathbf{3}^{2+}$ does exist in **1a-s**. While for the synthesis of **1b** and **1c** under solvothermal conditions, both yields are lower than that of **1a**, which means that only a small quantity of dioxygen existed in solvents and the vessel leads to the formation the SBUs of **1b** and **1c**, and thus there isn't any remnant $\mathbf{3}^{2+}$ in **1b-s** and **1c-s**. Once exposed to air, $\mathbf{3}^{2+}$ will soon generate (in **1b-s**) and thus can be detected by ESI-MS. However, it is still inexplicit why $\mathbf{3}^{2+}$ cannot form in **1c-s** that has been exposed to air for at least seven days (Fig. 4e). On the other hand, the formation of $\mathbf{3}^{2+}$ may also be related to the presence of ligand H_3BTB, because a DMF–EtOH solution of $CoCl_2$ having been stirred for more than one month in air (the color of solution has changed from blue to red) does not show evidence of $\mathbf{3}^{2+}$ (based on ESI-MS). Based on these points, we speculate that the transformation from **1a–1c** to **2** occurs as follows (Fig. 5): firstly, to crush the **1a–1c** crystals makes the diffusion of $\mathbf{3}^{2+}$ clusters into the 1D channels be feasible; then the incoming $\mathbf{3}^{2+}$ clusters trigger the cleavage of Co1–O1 and Co1–O2 bonds; and finally the $\mathbf{3}^{2+}$ clusters are bridged to the framework Co_3O units and the ancillary solvent molecules are replaced with the pendent carboxylate groups (O1 and O2). It should be noticed that whatever the terminal molecules on Co2 in **1a–1c** are, on Co2 in **2** they are water molecules. Meanwhile, Co1–O1W bonds (the bridging water molecule) in **1a** or **1b** may dissociate during the cleavage of Co1–O1 and Co1–O2 bonds.

Iodine uptake

Though complexes **1a–1c** are highly porous, they became amorphous upon heating or activation by supercritical CO_2 (SCD), so we could not investigate their sorption properties. In contrast, complex **2** could maintain crystallinity upon

activation by SCD (Fig. 6). When samples of **2** were activated by SCD, they turned into dark pink products **2′** (Fig. 7a), which further became purple products **2″** after storage in a desiccator containing solid NaOH for two days (Fig. 7b). Their capabilities for iodine adsorption were then tested. After immersion in cyclohexane solution of I_2 for three days (Fig. 7d and e), both products (**2′** and **2″**) became brown, which could not return to the original color when washed with cyclohexane. Meanwhile, the cyclohexane solution turned to light red, which indicates that iodine in the solution was adsorbed by the activated samples.[18–20] The iodine uptake by **2′** and **2″** were also examined by sublimation method, the gravimetric measurements[18d] taken at various time intervals during the iodine loading revealed that the mass of **2′** increased by 16.2 wt% after 240 h (Fig. 8), while that of **2″** increased significantly by 38.6 wt% after 240 h. That the sorption does not saturate for **2″** in the presence of excess iodine indicates continued deposition onto the crystal surface. The mass uptake of iodine by **2″** is comparable to the zeolite 13X[25] and the porous organic cage CC3.[19] After gravimetric measurements, both **2′** and **2″** changed to black crystalline products (**2‴**, Fig. 7c), and UV-Vis spectra in the solid states showed peaks associated with both samples (**2′** and **2″**) and iodine (Fig. 9). However, if **2** was activated by SCD and then pumped in vacuum, the framework might decompose or collapse (Fig. 6) and therefore hardly adsorbed iodine molecules. As shown in Fig. 8, the slight mass increase up to 2% may be merely due to the surface loading. This distinct difference in iodine uptake between samples of **2** after SCD reveals the different efficacy of post-SCD sample-manipulating methods.

Conclusions

In summary, we have reported an unexpected SCSC transformation through vigorous changes of SBUs, which is specifically triggered by postsynthetic uptake of free Co_3O species that are firstly proved to be substantive before being assembled into frameworks; the transformation simultaneously involves the cleavage and formation of Co–O bonds, the change of metal-to-ligand ratio and the tremendous change of MOF structures. Although many metal clusters have been utilized as SBUs to deconstruct MOFs for the purpose of structural analysis, the direct *in situ* synthesis of a specific SBU is still very difficult. Therefore, the present synthesis and/or adoption of "real" SBUs provides a true route to construct SBU-based MOF materials. On the other hand, coupled with the capability of capturing iodine by MOF **2**, the present case may also represent a new type of SCSC transformation and PSM that is able to tune structures and physicochemical properties of MOFs in the solid states.

Acknowledgements

This work was financially supported by the NNSF of China (21021061 & 20923004) and the Specialized Research Fund for the Doctoral Program of Higher Education (20110121110012).

Notes and references

1 (*a*) L. J. Murray, M. Dinca and J. R. Long, *Chem. Soc. Rev.*, 2009, **38**, 1294; (*b*) H. Bux, F. Y. Liang, Y. S. Li, J. Cravillon, M. Wiebcke and J. Caro, *J. Am. Chem. Soc.*, 2009, **131**, 16000; (*c*) D. Saha, Z. B. Bao, F. Jia and S. G. Deng, *Environ. Sci. Technol.*, 2010, **44**, 1820; (*d*) O. M. Yaghi, M. O'Keeffe, N. W. Ockwig, H. K. Chae, M. Eddaoudi and J. Kim, *Nature*, 2003, **423**, 705.

2 (*a*) J. Lee, O. K. Farha, J. Roberts, K. A. Scheidt, S. T. Nguyen and J. T. Hupp, *Chem. Soc. Rev.*, 2009, **38**, 1450; (*b*) H. H. Fei, D. L. Rogow and S. R. J. Oliver, *J. Am. Chem. Soc.*, 2010, **132**, 7202; (*c*) F. Gándara, B. Gomez-Lor, E. Gutiérrez-Puebla, M. Iglesias, M. A. Monge, D. M. Proserpio and N. Snejko, *Chem. Mater.*, 2008, **20**, 72.

3 M. D. Allendorf, C. A. Bauer, R. K. Bhakta and R. J. T. Houk, *Chem. Soc. Rev.*, 2009, **38**, 1330.

4 (*a*) P. Horcajada, C. Serre, M. Vallet-Regi, M. Sebban, F. Taulelle and G. Férey, *Angew. Chem., Int. Ed.*, 2006, **45**, 5974; (*b*) P. Horcajada, T. Chalati, C. Serre, B. Gillet, C. Sebrie, T. Baati, J. F. Eubank, D. Heurtaux, P. Clayette, C. Kreuz, J. S. Chang, Y. K. Hwang, V. Marsaud, P. N. Bories, L. Cynober, S. Gil, G. Férey, P. Couvreur and R. Gref, *Nat. Mater.*, 2010, **9**, 172.

5 (*a*) B. V. Harbuzaru, A. Corma, F. Rey, P. Atienzar, J. L. Jorda, H. Garcia, D. Ananias, L. D. Carlos and J. Rocha, *Angew. Chem., Int. Ed.*, 2008, **47**, 1080; (*b*) K. C. Stylianou, R. Heck, S. Y. Chong, J. Bacsa, J. T. A. Jones, Y. Z. Khimyak, D. Bradshaw and M. J. Rosseinsky, *J. Am. Chem. Soc.*, 2010, **132**, 4119.

6 (*a*) G. J. Halder, C. J. Kepert, B. Moubaraki, K. S. Murray and J. D. Cashion, *Science*, 2002, **298**, 1762; (*b*) M.-H. Zeng, M.-X. Yao, H. Liang, W.-X. Zhang and X.-M. Chen, *Angew. Chem., Int. Ed.*, 2007, **46**, 1832.

7 (*a*) B. L. Chen, M. Eddaoudi, S. T. Hyde, M. O'Keeffe and O. M. Yaghi, *Science*, 2001, **291**, 1021; (*b*) X. Lin, J. Jia, X. Zhao, K. Thomas, A. Blake, G. Walker, N. R. Champness, P. Hubberstey and M. Schröder, *Angew. Chem., Int. Ed.*, 2006, **45**, 7358; (*c*) H. Furukawa, J. Kim, N. W. Ockwig, M. O'Keeffe and O. M. Yaghi, *J. Am. Chem. Soc.*, 2008, **130**, 11650.

8 (*a*) H. K. Chae, D. Y. Siberio-Perez, J. Kim, Y. Go, M. Eddaoudi, A. J. Matzger, M. O'Keeffe and O. M. Yaghi, *Nature*, 2004, **427**, 523; (*b*) K. Koh, A. G. Wong-Foy and A. J. Matzger, *Angew. Chem., Int. Ed.*, 2008, **47**, 677.

9 A. C. Sudik, A. R. Millward, N. W. Ockwig, A. P. Côté, J. Kim and O. M. Yaghi, *J. Am. Chem. Soc.*, 2005, **127**, 7110.

10 (*a*) Y.-B. Zhang, W.-X. Zhang, F.-Y. Feng, J.-P. Zhang and X.-M. Chen, *Angew. Chem., Int. Ed.*, 2009, **48**, 5287; (*b*) A. Schoedel, L. Wojtas, S. P. Kelley, R. D. Rogers, M. Eddaoudi and M. J. Zaworotko, *Angew. Chem., Int. Ed.*, 2011, **50**, 11421; (*c*) A. Vimont, J. M. Goupil, J. C. Lavalley, M. Daturi, S. Surblé, C. Serre, F. Millange, G. Férey and N. Audebrand, *J. Am. Chem. Soc.*, 2006, **128**, 3218; (*d*) A. C. Sudik, A. P. Côté and O. M. Yaghi, *Inorg. Chem.*, 2005, **44**, 2998.

11 (*a*) C. Hu and U. Englert, *Angew. Chem., Int. Ed.*, 2005, **44**, 2281; (*b*) S. K. Ghosh, J.-P. Zhang and S. Kitagawa, *Angew. Chem., Int. Ed.*, 2007, **46**, 7965; (*c*) G. Mahmoudi and A. Morsali, *Cryst. Growth Des.*, 2008, **8**, 391.

12 (*a*) H. Konaka, L. P. Wu, M. Munakata, T. Kuroda-Sowa, M. Maekawa and Y. Suenaga, *Inorg. Chem.*, 2003, **42**, 1928; (*b*) G. Georgiev and L. R. MacGillivray, *Chem. Soc. Rev.*, 2007, **36**, 1239; (*c*) P. B. Chatterjee, A. Audhya, S. Bhattacharya, S. M. T. Abtab, K. Bhattacharya and M. Chaudhury, *J. Am. Chem. Soc.*, 2010, **132**, 15842.

13 (*a*) L. Iordanidis and M. G. Kanatzidis, *J. Am. Chem. Soc.*, 2000, **122**, 8319; (*b*) H. J. Choi and M. P. Suh, *J. Am. Chem. Soc.*, 2004, **126**, 15844.

14 (*a*) M. C. Das and P. K. Bharadwaj, *J. Am. Chem. Soc.*, 2009, **131**, 10942; (*b*) M. H. Mir and J. J. Vittal, *Cryst. Growth Des.*, 2008, **8**, 1478.

15 B. Li, R.-J. Wei, J. Tao, R.-B. Huang, L.-S. Zheng and Z.-P. Zheng, *J. Am. Chem. Soc.*, 2010, **132**, 1558.

16 (*a*) S. M. Cohen, *Chem. Rev.*, 2012, **112**, 970; (*b*) Z. Zhang, L. Zhang, L. Wojtas, P. Nugent, M. Eddaoudi and M. J. Zaworotko, *J. Am. Chem. Soc.*, 2012, **134**, 924; (*c*) T. Haneda, M. Kawano, T. Kawamichi and M. Fujita, *J. Am. Chem. Soc.*, 2008, **130**, 1578.

17 (*a*) J. S. Costa, P. Gamez, C. A. Black, O. Roubeau, S. J. Teat and J. Reedijk, *Eur. J. Inorg. Chem.*, 2008, 1551; (*b*) Z. Wang, K. K. Tanabe and S. M. Cohen, *Inorg. Chem.*, 2009, **48**, 296; (*c*) J. Canivet, S. Aguado, C. Daniel and D. Farrusseng, *ChemCatChem*, 2011, **3**, 675; (*d*) K. Kim, S. J. Garibay and S. M. Cohen, *Inorg. Chem.*, 2011, **50**, 729; (*e*) M. Banerjee, S. Das, M. Yoon, H. J. Choi, M. H. Hyun, S. M. Park, G. Seo and K. Kim, *J. Am. Chem. Soc.*, 2009, **131**, 7524.

18 (*a*) D. F. Sava, M. A. Rodriguez, K. W. Chapman, P. J. Chupas, J. A. Greathouse, P. S. Crozier and T. M. Nenoff, *J. Am. Chem. Soc.*, 2011, **133**, 12398; (*b*) Q.-K. Liu, J.-P. Ma and Y.-B. Dong, *Chem. Commun.*, 2011, **47**, 7185; (*c*) K. W. Chapman, D. F. Sava, G. J. Halder, P. J. Chupas and T. M. Nenoff, *J. Am. Chem. Soc.*, 2011, **133**, 18583; (*d*) M. Liu, W.-P. Liao, C.-H. Hu, S.-C. Du and H.-J. Zhang, *Angew. Chem., Int. Ed.*, 2012, **51**, 1585; (*e*) L. Chen, K. Tan, T.-Q. Lan, S.-L. Li, K.-S. Shao and Z.-M. Su, *Chem. Commun.*, 2012, **48**, 5919.

19 T. Hasell, M. Schmidtmann and A. I. Cooper, *J. Am. Chem. Soc.*, 2011, **133**, 14920.

20 (*a*) M.-H. Zeng, Q.-X. Wang, Y.-X. Tan, S. Hu, H.-X. Zhao, L.-S. Long and M. Kurmoo, *J. Am. Chem. Soc.*, 2010, **132**, 2561; (*b*) Z. Yin, Q.-X. Wang and M.-H. Zeng, *J. Am. Chem. Soc.*, 2012, **134**, 4857.

21 R. Ohtani, K. Yoneda, S. Furukawa, N. Horike, S. Kitagawa, A. B. Gasper, M. C. Muñoz, J. A. Real and M. Ohba, *J. Am. Chem. Soc.*, 2011, **133**, 8600.

22 S.-Q. Ma and H.-C. Zhou, *J. Am. Chem. Soc.*, 2006, **128**, 11734.

23 A. L. Spek, *PLATON, A Multipurpose Crystallographic Tool*, Utrecht University, Utrecht, The Netherlands, 2001.

24 E. J. de Hoffmann, *J. Mass Spectrom.*, 1996, **31**, 129.

25 M. Murthi and R. Q. Snurr, *Langmuir*, 2004, **20**, 2489.

26 (*a*) P. Wollmann, M. Leistner, U. Stoeck, R. Grunker, K. Gedrich, N. Klein, O. Throl, W. Grahlert, I. Senkovska, F. Dreisbach and S. Kaskel, *Chem. Commun.*, 2011, **47**, 5151; (*b*) K. Barthelet, J. Marrot, D. Riou and G. Férey, *Angew. Chem., Int. Ed.*, 2002, **41**, 281.

